

1
2
3
4
5
6
7
8
9
10
11
12
13
14
15
16
17
18
19
20
21
22
23
24
25
26
27
28
29
30

Abnormality of the placental vasculature affects placental thickness.

Michael Yampolsky¹, Carolyn M. Salafia^{2,3}, Oleksandr Shlakhter⁴,

Danielle Haas², Barbara Eucker⁵, John Thorp⁵

¹ Department of Mathematics, University of Toronto, 40 St. George St, Toronto, Ontario, Canada, M5S2E4

² Placental Analytics, LLC, Larchmont, NY, USA

³ Department of Obstetrics and Gynecology and Pediatrics, New York Methodist Hospital, Brooklyn, NY.

⁴ Rotman School of Management, University of Toronto, 105 St. George Street, Toronto, ON, M5S 3E6, Canada

⁵ Department of Obstetrics and Gynecology, University of North Carolina, Chapel Hill, Chapel Hill, North Carolina.

Corresponding author:
Michael Yampolsky, PhD
Department of Mathematics
University of Toronto
40 St. George Street, Toronto, Canada M5S2E4
Email: yampolsky.michael@gmail.com

31 **Abstract.**

32 **Background.** Our empirical modeling suggests that deformation of placental vascular growth is
33 associated with abnormal placental chorionic surface shape. Altered chorionic surface shape is
34 associated with lowered placental functional efficiency. We hypothesize that placentas with
35 deformed chorionic surface vascular trees and reduced functional efficiency also have irregular
36 vascular arborization that will be reflected in increased variability of placental thickness and a
37 lower mean thickness.

38 **Materials and Methods.** The sample was drawn from the *Pregnancy, Infection, and Nutrition*
39 *Study*, a cohort in which 94.6 percent of women consented to placental examination. Of these,
40 87% had placentas collected and photographed for chorionic surface analysis. Of the 1023
41 delivered at term, intact placentas were fixed, sliced and photographed in 587 (57%) cases..
42 Fourier analysis was used to quantify the non-centrality of the umbilical cord insertion, and
43 regularly irregular chorionic surface shapes. To quantify the disk thickness, one slice of the
44 placenta at the mid-section was used to calculate the mean and variance of placental thickness.
45 Functional efficiency was quantified as the scaling exponent $\beta = \log(\text{Placental Weight}) / \log(\text{Birth}$
46 $\text{Weight, normally } 0.75)$ with higher β corresponding to lower functional efficiency. Spearman's
47 correlations considered $p < 0.05$ significant.

48 **Results.** Non-centrality of the umbilical cord insertion was strongly and significantly positively
49 correlated with disk thickness of the (Spearman's $\rho = 0.128$, $p = 0.002$). Deformed shape was
50 strongly and significantly associated with lower overall thickness and higher variability of
51 thickness with ρ between -0.173 and -0.254 ($p < 0.001$) . Both lower mean thickness and high
52 variability of thickness are strongly correlated with higher β (reduced placental efficiency)
53 ($p < 0.001$ and $p = 0.038$ respectively). Greater thickness variability is correlated with higher β
54 independent of the other placental shape variables $p = 0.004$.

55 **Conclusions.** Our findings confirm the predictions of our empirical modeling. A regularly
56 deformed placental surface is associated with non-uniform placental thickness and lower
57 average thickness. We speculate that lower mean thickness or high variability of thickness are
58 caused by variable villous arborization due to abnormal placental vascular growth. Supporting
59 this, placentas with lower average thickness or higher variability of thickness are less
60 functionally efficient. Variability of placental disk thickness, even when restricted to analysis of a
61 single random diameter, is particularly useful as an independent indicator of lowered placental
62 efficiency, and thus abnormal placental vascular growth.

63

64 Keywords: Placenta, placental weight, placental thickness, birth weight, placental function,
65 chorionic plate

66

67 **Introduction.**

68 In our previous work [1,2] we described how a deformation of the placental vascular growth is
69 reflected in an abnormal placental surface shape and reduced placental functional efficiency.
70 Commonly, when the angiogenesis of the vascular tree is impacted in our model [1], the growth
71 of the branches of the vascular tree is depressed below a certain level. This results in a model
72 tree with gaps in the vascular coverage concentrated in sectors between larger vascular
73 branches. The placental surface will typically be deformed into a commonly observed “regularly-
74 irregular” multilobate or star-like shape. We have conjectured that the gaps in the vascular
75 penetration by a deformed vascular tree will also lead to an increased variability of placental
76 cross-sectional thickness and lowered overall thickness. Reduced vascular arborization, is in
77 turn associated with lower placental functional efficiency, as shown in [2].

78 In the present work we test these hypotheses by analyzing the relation of the placental
79 thickness, measured in a single randomly oriented cross-section through the center of the
80 placental surface, with the placental shape. We use Fourier analysis to quantify the shape of the
81 chorionic plate, since it can quantify the typical “regularly-irregular” placental shapes described
82 in [1].

83 If variable thickness does in fact reflect variable villous arborization and, by extension,
84 vascularity, then variability of placental thickness would also be expected to have an effect on
85 the placental functional efficiency, quantified as the fetoplacental scaling exponent β [3,4].

86 To test our methods of measuring placental thickness, we can apply them to study the impact of
87 non-centrality of umbilical cord insertion on thickness. As shown in [2], non-central insertion is
88 not associated with a change in placental surface shape, and is significantly correlated with a
89 larger placental weight, and lower functional efficiency (smaller baby for a given placental
90 weight). We thus expect to find that a non-centrality of cord insertion produces a measurable

91 increase in placental thickness, which for the same surface area would result in a heavier
92 placenta.

93 **Materials and Methods.**

94 *Placental Cohort*

95 The *Pregnancy, Infection, and Nutrition Study* is a cohort study of pregnant women recruited at
96 mid pregnancy from an academic health center in central North Carolina. Our study population
97 and recruitment techniques are described in detail elsewhere [5]. Beginning in March 2002, all
98 women recruited into the *Pregnancy, Infection, and Nutrition Study* were requested to consent
99 to a detailed placental examination. As of October 1, 2004, 94.6 percent of women consented
100 to such examination. Of those women who consented, 87 percent had placentas collected and
101 photographed for image analysis. Of the 1,225 consecutive placentas collected, 1023 were
102 delivered at term. Placental gross examinations, histology review, and image analyses were
103 performed at *EarlyPath Clinical and Research Diagnostics*, a New York State-licensed
104 histopathology facility under the direct supervision of Dr. Salafia. The Institutional Review Board
105 of the University of North Carolina at Chapel Hill approved this protocol.

106

107 The fetal surface of the placenta was wiped dry and placed on a clean surface after which the
108 extraplacental membranes and umbilical cord were trimmed from the placenta. The fetal
109 surface was photographed with the Lab ID number and 3 cm. of a plastic ruler in the field of
110 view using a standard high-resolution digital camera (minimum image size 2.3 megapixels). A
111 trained observer (D.H.) captured series of x,y coordinates that marked the site of the umbilical
112 cord insertion, the perimeter of the fetal surface, and the “vascular end points”, the sites at
113 which the chorionic vessels disappeared from the fetal surface. The perimeter coordinates were

114 captured at intervals of between 1cm and 2cm, and more coordinates were captured if it
115 appeared essential to accurately capturing the shape of the fetal surface.

116

117 Placentas were cut perpendicularly to the chorionic plate by a series of parallel cross-sections.
118 The cuts were generally made starting from the apparent geometric center towards the edge of
119 the placental surface creating 8 slices and 7 unique cross-sections. The frequency of the cross-
120 sections was increased if it appeared necessary to capture significant details of placental shape,
121 such as multiple lobes. Each placental slice was digitally traced by a trained observer (D.H.) to
122 capture its perimeter. The perimeter coordinates were again captured at intervals of between 1
123 and 2cm.

124

125 Placentas which were received from the Pathology Department in several pieces, or with parts
126 removed could not be sliced according to the protocol. This has resulted in a reduced number of
127 cut placentas, compared to the number of placentas collected. The total number of placentas for
128 which the traced slices were obtained is 771, of which N=587 were delivered at term. This
129 equals 57% of all placentas delivered at term in the study.

130

131 *Fourier analysis of the placental surface shape.*

132 As in our previous work [2], we use Fourier analysis to quantify the placental surface shape.
133 First, the umbilical insertion point is placed at the origin. Perimeter markers are connected by
134 straight line segments to obtain an approximate perimeter P of the chorionic plate. A sector of
135 opening of 6° with vertex at the origin is rotated in 6° increments. For each turn of the sector, the
136 points in P inside of it are averaged to yield a radial marker. In this way, we obtain 60 radii
137 emanating from the origin spaced at 6° intervals. They are connected to obtain the *angular*

138 *radius* $r(\theta)$, which is a function of the angle θ from the umbilical insertion point. For the function
139 $r(\theta)$ we compute its Fourier coefficients C_n as

$$C_n = \frac{1}{2\pi} \int_0^{2\pi} e^{-in\theta} r(\theta) d\theta$$

140 Fourier coefficients are a useful tool, in particular, since we would like to identify the typical
141 regularly-irregular placental surface shapes, such as tri-lobate, and star-shaped placentas (see
142 Fig. 1 and Fig 2). An n -fold symmetry of the placental surface is reflected in a larger value of
143 the coefficient C_n . In Fig. 3 we demonstrate this principle with two idealized placental shapes: a
144 tri-lobate one ($C_3=1$, and for all other $n>0$, $C_n=0$), and a star-shaped one ($C_5=1$, and for all other
145 $n>0$, $C_n=0$). Observe, how this principle works for also for real regularly-irregular placentas in
146 Fig 1.

147 *Quantifying the displacement of the umbilical cord insertion.*

148 We have shown in [2] that the centrality of the insertion of the umbilical cord has a significant
149 impact on the placental functional efficiency. As in [2], we use the Fourier coefficient C_1 to
150 measure the non-centrality of the insertion, and call it the *Fourier displacement* of the umbilical
151 cord. If the shape is circular, with a central cord insertion, then $C_1=0$. A large Fourier
152 displacement of the umbilical cord insertion does not influence the normal round shape and of a
153 normal diameter. However, a large displacement results in a heavier placenta [2], with a
154 reduced functional efficiency per unit of placental mass: larger β , which means a smaller baby
155 for a given placental weight.

156

157 *Quantifying the abnormality of placental surface shape and deformation of placental vascular*
158 *tree.*

159 We use Fourier coefficients C_2, C_3, C_4, C_5 to describe the variability of the shape of the placental
160 surface. Our DLA (Diffusion Limited Aggregation) stochastic growth model of placental

161 vasculature [1] predicts that a deformed surface shape reflects an abnormal development of the
162 placental vascular tree. Typical deformations of the vascular growth described in [1] result in
163 star-shaped or multi-lobate placentas. Quantitatively, such a placental shape has large values of
164 C_2, C_3, C_4, C_5 . The size of the coefficient reflects the symmetry of the placental shape; e.g. a tri-
165 lobate placenta will have a larger C_3 (see Figure 1).

166 We also use a measurement of deviation of placental shape from the mean round shape
167 described in [7] as *Symmetric Difference* Δ . The larger value of Δ implies a larger difference
168 between the placental surface area and the mean round shape.

169 Our DLA model predicts that the vasculature of a regularly-irregular shaped placenta fills the
170 surface unevenly [1 4], with gaps in vascular coverage forming sectors centered on the umbilical
171 insertion point. This would produce a cross-section of a highly variable thickness, with thinner
172 areas corresponding to the sectors with less vascular coverage.

173

174 *Quantifying the placental thickness.*

175 To measure placental thickness, we analyze the *central* cross-cut of the placenta, which
176 approximates the longer placental diameter. We parameterize the top and bottom boundaries of
177 the central slice by their length. We then put 100 markers on top and bottom of the slice so that
178 the length of the boundary piece between two markers is constant. The markers are grouped
179 into opposite pairs.

180 We measure the following quantities:

- 181 a) *mean placental thickness* is the mean distance between the opposing markers;
- 182 b) *normalized mean placental thickness* is the mean placental thickness divided by the
183 width of the slice;
- 184 c) *variability of thickness* for each pair of opposite markers $Marker_i^{top}, Marker_i^{bottom}$ we
185 calculate $d_i = \text{distance}(Marker_i^{top}, Marker_i^{bottom})$, which is the thickness of the slice

186 measured between the two markers. We then calculate the absolute value of the
187 deviation of d_i from from mean placental thickness. We average the deviations over all
188 pairs of markers, and divide the resulting quantity by the value of the mean placental
189 thickness. The result is a number between 0 and 1, with 0 corresponding to no variability
190 (uniform thickness).

191 *Measuring placental functional efficiency.*

192 As we have shown in [3,4] the birth weight of a newborn (BW) does not scale linearly with the
193 placental weight (PW). The scaling relation between the two quantities is

194
$$PW \sim BW^{3/4},$$

195 which is a version of Kleiber's Law, reflecting the fractal structure of the placental vasculature.

196 We have introduced a measure of the placental functional efficiency

197
$$\beta = \log PW / \log BW.$$

198 A larger value of β corresponds to a lower birth weight for a given placental weight, and hence a
199 lowered placental function per unit of volume.

200 *Software.*

201 Numerical simulations of vascular trees were carried out using our ANSI C, 3-dimensional,
202 diffusion-limited aggregation simulation package "*DLA-3d-placenta*", developed under the terms
203 of the GNU General Public License as published by Free Software Foundation. For DLA cluster
204 visualization we have used *PovRay*: a freeware ray tracing program available for a variety of
205 computer platforms. Fourier coefficients were calculated using *Maplesoft Maple 12.0*
206 Mathematics and Engineering software. The analysis of the digitally traced placental surfaces
207 and slices was carried out using our proprietary ANSI C package "Placental-geometry".

208 **Results.**

209 *Thickness versus Fourier displacement.*

210 The first Fourier coefficient C_1 is strongly and significantly *positively* correlated with mean
211 thickness (Pearson's $r=0.146$, $p<0.001$; Spearman's $\rho=0.128$, $p=0.002$). Thus a large umbilical
212 cord displacement results in a thicker placenta. This confirms the findings of [2].

213

214 *Variability of thickness versus variability of the shape.*

215 Our present measurements support the predictions of the DLA model [1], see Figure 2. The
216 coefficients C_2 , C_3 , C_4 , C_5 are strongly and significantly correlated with the variability of
217 thickness (see Table 1). Further, there is a negative correlation with mean thickness, and with
218 normalized mean thickness. Thus, the deformation of the placental surface shape which
219 corresponds to a deformed placental vascular growth, (which may, in particular, be manifested
220 as a regularly-irregular shape), results in a higher variability of placental thickness, and a lower
221 mean thickness.

222

223 *Variability of thickness versus placental efficiency.*

224 Finally, we test whether the effect of the lower placental thickness is a reduced placental
225 efficiency, as predicted by our model [1,4]. We find a strong and significant *positive* correlation
226 of variability of thickness with β . Thus, a placenta with thin parts will tend to have a reduced
227 functional efficiency, resulting in a smaller baby for a given placental weight.

228 Using the symmetric difference Δ , thickness, and umbilical cord displacement as control
229 variables, we find a significant ($p<0.004$) partial correlation (0.135) between the value of β and
230 variability of thickness.

231 **Conclusions.**

232 Our findings confirm the predictions of the empirical model of placental vascular growth [1,2], as
233 well as demonstrate the effectiveness of Fourier analysis of the placental chorionic surface
234 shape. We find two distinct scenarios in which the morphology of the placental surface affects

235 the placental thickness. In the first, the umbilical cord is inserted non-centrally. As shown in [2],
236 there is no abnormality in the placental surface shape in this case. Yet, there is an increase in
237 the placental weight, relative to the birth weight. This is confirmed by our present results, which
238 show a higher average thickness of the placenta in this case. The placental functional efficiency
239 is lowered, which is reflected in a higher value of the scaling exponent β .

240 The second scenario corresponds to a deformed placental surface shape, quantified as a higher
241 value of one of the Fourier coefficients C_2, \dots, C_5 . This case includes, in particular, the typical
242 regularly-irregular placental shapes, such as multi-lobate or star-shaped placentas. We have
243 speculated [1] that these deformed shapes reflect irregular villous arborization due to the impact
244 of stressors on the placental vascular branching growth. We have proposed in [1], based on our
245 empirical model of placental vascular growth, that such surface shapes will be accompanied by
246 irregular placental thickness, with thinner areas corresponding to gaps in vascular coverage.
247 This is confirmed by the findings of the present paper. Deformed surface shapes correspond to
248 highly variable thickness. The presence of areas of low thickness leads to a lower average
249 thickness in this case. As expected [1,4], such placentas also have a lowered functional
250 efficiency (a higher value of β), and thus yield a smaller baby for a given placental weight.

251

252 Accounting for effects of placental shape, cord displacement, and the value of thickness as
253 factors, we see that the variability of thickness alone is responsible for much of the observed
254 reduction in placental functional efficiency. Thus, the non-uniform villous and vascular
255 arborization, which is reflected in a non-uniformly thick placenta, is reflected in a lower birth
256 weight for a given placental weight (larger β).

257 The measurement of variability of placental thickness is thus shown to be a valuable predictor
258 of placental functional efficiency, reflecting deficiencies of placental vascular development which
259 may not be detectable from the placental surface shape.

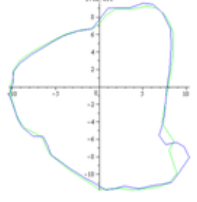
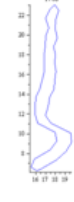
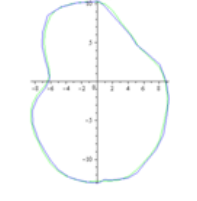
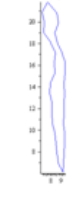
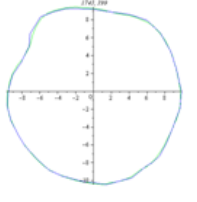
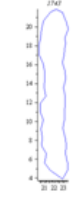
260 Our approach to the study of placental thickness has been motivated by the qualitative modeling
261 of the fractal growth of the placental vasculature started in [1]. Other authors have studied the
262 fractal structure of the placental vascular tree and its impact on the placental function (e.g.
263 [8,9,10]). We expect this approach to yield further insights.

264 This work was partially supported by NSERC Discovery Grant (M. Yampolsky), by NARSAD
265 Young Investigator Award (C. Salafia), by K23 MidCareer Development Award NIMH
266 K23MH06785 (C. Salafia).

267

268 **Figure 1: placental shape and thickness.** (a) tri-lobate placenta: large C_3 , small mean
 269 thickness; (b) bi-lobate placenta: large C_2 , small mean thickness; (c) normally shaped placenta.

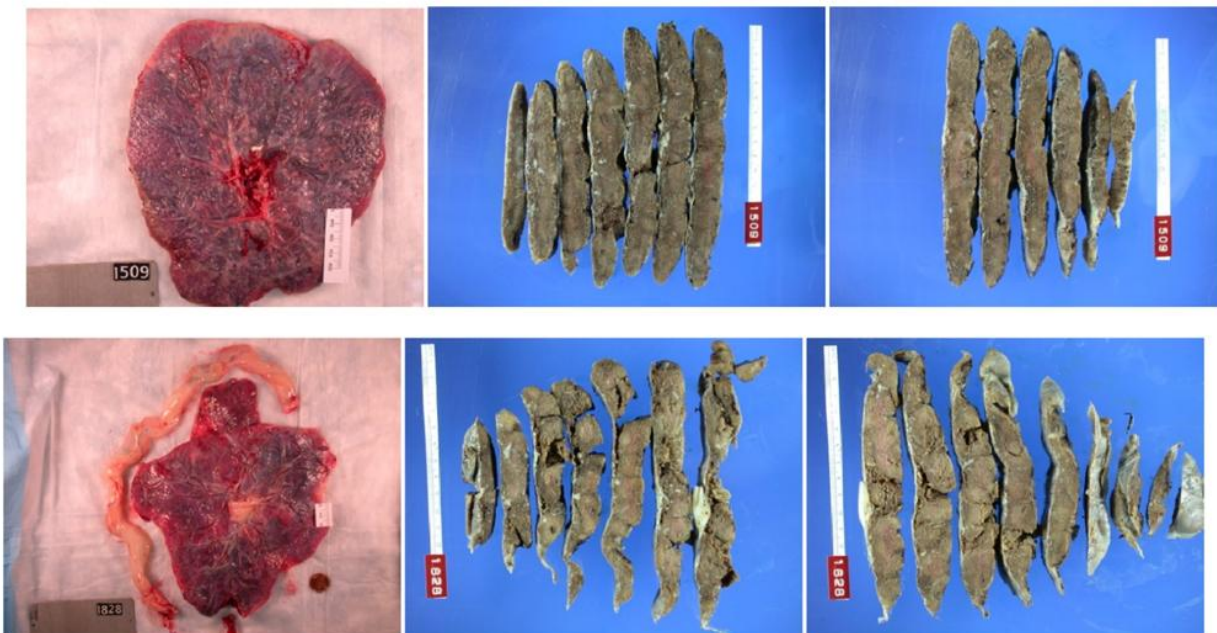
270

Traced placental perimeter	Traced central slice	Fourier coefficients	Mean thickness	Normalized mean thickness
(a) 		$C_1=1.57$ $C_2=0.80$ $C_3=1.42$ $C_4=0.7$ $C_5=0.25$	1.134	0.071
(b) 		$C_1=1.78$ $C_2=2.18$ $C_3=1.07$ $C_4=0.39$ $C_5=0.38$	1.005	0.072
(c) 		$C_1=0.64$ $C_2=0.49$ $C_3=0.34$ $C_4=0.46$ $C_5=0.28$	2.243	0.134

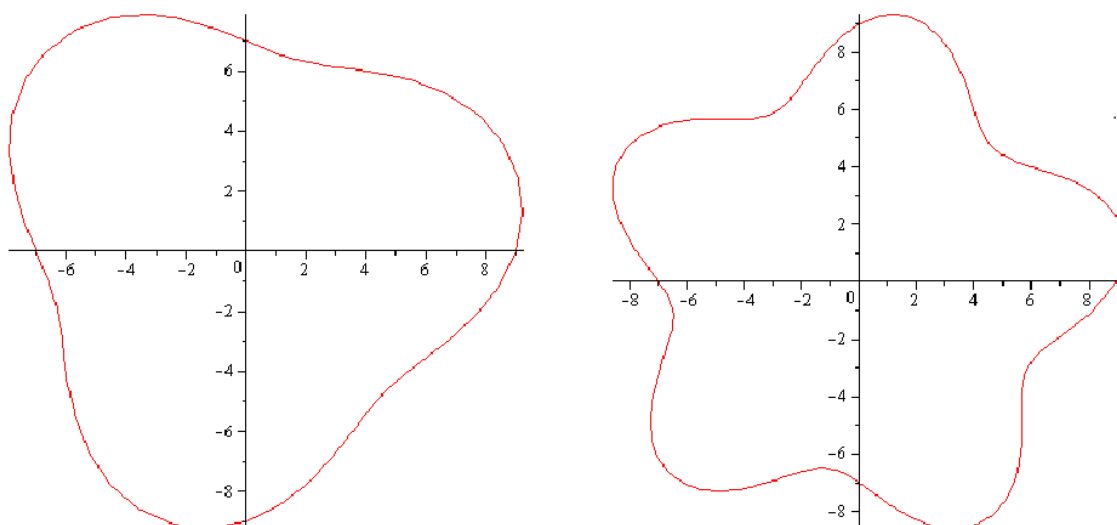
271

272

273 **Figure 2: variability of thickness for irregularly-shaped placentas described by the DLA**
 274 **model.** Above: the slices of a round placenta have uniform thickness. Below: the slices of a star-
 275 shaped placentas have highly variable thickness.



276
 277 **Figure 3: idealized placental shapes and Fourier coefficients.** Left: idealized tri-lobate
 278 placenta, $C_3=1$, for all other $n>0$, $C_n=0$. Right: idealized star-shaped placenta, $C_5=1$, for all other
 279 $n>1$, $C_n=0$.



280
 281

282 **Table 1. Correlations of Fourier coefficients with thickness variables.**

	C₁	C₂	C₃	C₄	C₅	β
Mean thickness	r=0.146 (p<0.001) ρ=0.128 (p =0.002)	r=-0.91 (p=0.028) ρ=-0.76 (p=0.66)	r=-0.172 (p<0.001) ρ=-0.135 (p=0.001)	r=-0.184 (p <0.001) ρ=-0.185 (p <0.001)	r=-0.145 (p <0.001) ρ=-0.114 (p =0.006)	r=0.454 (p<0.001) ρ=0.467 (p <0.001)
Normalized mean thickness	r=0.064 (p =0.121) ρ=0.060 (p =0.147)	r=-0.189 (p<0.001) ρ=-0.175 (p <0.001)	r=-0.267 (p <0.001) ρ=-0.214 (p<0.001)	r=-0.244 (p <0.001) ρ=-0.234 (p <0.001)	r=-0.222 (p <0.001) ρ=-0.173 (p<0.001)	r=0.210 (p<0.001) ρ=0.254 (p<0.001)
Variability of thickness	r=0.102 (p=0.013) ρ=0.101 (p=0.014)	r=0.114 (p=0.006) ρ=0.057 (p =0.171)	r=0.154 (p <0.001) ρ=0.111 (p=0.007)	r=0.149 (p<0.001) ρ=0.102 (p =0.013)	r=0.146 (p<0.001) ρ=0.081 (p =0.050)	r=0.076 (p =0.065) ρ=0.086 (p=0.038)

283

284

285

286 References

287 1. M. Yampolsky, C. Salafia, O. Shlakter, D. Haas, B. Eucker, J. Thorp. [Modeling the variability](#)
288 [of shapes of a human placenta](#), Placenta, 29(2008), 790 – 797.

289 2. M. Yampolsky, C. Salafia, O. Shlakter, D. Haas, B. Eucker, J. Thorp. [Centrality of the](#)
290 [umbilical cord insertion in a human placenta influences the placental efficiency](#), Placenta, 30
291 (2009) 1058-1064.

292 3. Salafia CM, Misra DP, Yampolsky M, Charles AK, Miller RK. [Allometric metabolic scaling](#)
293 [and fetal and placental weight](#), Placenta, 30(2009), 355-360.

294 4. Salafia CM, Yampolsky M. [Metabolic scaling law for fetus and placenta](#), Placenta, 30(2009),
295 468-471.

296 [5] Savitz DA, Dole N, Williams J, et al. Determinants of participation in an epidemiological study
297 of preterm delivery. Paediatr Perinat Epidemiol 1999;13:114–25

298 [6] <http://www.cpc.unc.edu/projects/pin>

299 [7] M. Yampolsky, O. Shlakter, C. Salafia, D. Haas. [Mean surface shape of a human placenta](#),
300 e-print Arxiv.org, 0807.2995

301 [8] [Bergman DL](#), [Ullberg U](#). Scaling properties of the placenta's arterial tree. J Theor Biol. 1998
302 Aug 21;193(4):731-8.

303 [9] [Wielgus E](#), [Pawlicki K](#), [Kawa A](#), [Włoch S](#), [Kamiński M](#). Fractal analysis of placenta mature
304 villi in healthy, smoking and non-smoking women. Med Sci Monit. 2000 Mar-Apr;6(2):271-7.

305 [10] [Kikuchi A](#), [Unno N](#), [Shiba M](#), [Sunagawa S](#), [Ogiso Y](#), [Kozuma S](#), Multifractal description of
306 the maternal surface of the placenta. Gynecol Obstet Invest. 2008;66(2):127-33.